Electronic Supplementary Material (ESI) for Chemical Science.

Metal Substrate Catalysis In the Confined Space for Platinum Drug Delivery

Susana Velasco-Lozano[a], Silvia Alonso-de Castro,[b] Ana I. Benítez-Mateos,[a] Fernando López-Gallego,[a,c]* Luca Salassa[b,c,d]*

[a] *Center for Cooperative Research in Biomaterials (CIC biomaGUNE), Basque Research and Technology Alliance (BRTA), Paseo de Miramon 182, 20014, San Sebastián, Spain*
[b] *Donostia International Physics Center, Paseo Manuel de Lardizabal 4, Donostia, 20018, Spain*
[c] *Ikerbasque, Basque Foundation for Science, Bilbao, 48011, Spain*
[d] *Polimero eta Material Aurreratuak: Fisika, Kimika eta Teknologia, Kimika Fakultatea, Euskal Herriko Unibertsitatea UPV/EHU, Paseo Manuel de Lardizabal 3, Donostia, 20018, Spain*

Electronic Supplementary Material

Table of Contents

1. Materials and methods

Riboflavin 5′-monophosphate sodium salt hydrate (**FMN**), β-nicotinamide adenine dinucleotide reduced disodium salt hydrate (NADH), tris(hydroxymethyl)aminomethane (Tris) were purchased by Merk. K_2PtCl_4 was obtained by Precious Metals Online. Diethylaminoethyl agarose microbeads (**AGM**) were acquired from GE Healthcare. 8-well µslides were supplied by Ibidi.

Synthesis. The complex *cis,cis,trans*-$[Pt(NH_3)_2(Cl_2)(O_2CCH_2CH_2CO_2H_2)_2]$ was synthesized and characterized as previously reported.[1]

Loading of diethylaminoethyl agarose microbeads (AGM). Approximately 50 mg of **AGM** were prewashed three times by soaking and shaking (10 min) the microbeads in Tris buffer (10 mM, pH 7.6). Then, **1** (1 mM) and **FMN** (75 µM) were dissolved in Tris buffer separately and loaded sequentially on **AGM** by soaking and shaking the hydrogel material in 0.5 mL solutions of the two. At each step, suspensions of **AGM** were incubated in dark conditions for 10 min at 298 K and rotary mixed at 50 rpm. Then, the supernatant was filtered. **FMN** and **1** are both negatively charged at pH 7.6, hence apt to interact electrostatically with the diethylaminoethyl groups of **AGM** that are positively charge at such pH. Release of components at each loading was determined by washing **AGM** with 0.5 mL of Tris buffer after every reagent addition, and by subsequent filtering. Loading values of the components were determined by UV-Vis (absorbance at 240 and 445 nm) and UPLC-MS, estimating concentrations of **FMN** and **1,** respectively, that remained in the supernatant after soaking, shaking and filtering.
Glucose oxidase (GOX) immobilization. 10 volumes of GOX solution (1 mg of crude powder/mL, glucose oxidase type II from *Aspergillus Niger* > 10000 U/g solid, Sigma) were incubated with one volume of **AGM** microbeads during 10 min at 298 K. The immobilization yield was monitored by measuring the remaining GOX in the supernatant after filtration by the Bradford assay (data not shown). Afterwards, loading of **1** and the **FMN** was achieved as previously described with the only difference of a longer incubation for **1** (30 min instead of 10 min).

Nuclear Magnetic Resonance (NMR). ^{1}H NMR spectra of the various samples were recorded on a Fourier TM Bruker 300 NMR and on an AVANCE III Bruker 500 NMR spectrometer using standard pulse programs. Chemical shifts were reported in parts-per-million (δ, ppm) and referenced to the residual solvent peak.

UPLC-MS. Chromatography was performed in an Acquity UPLC system using an Acquity BEH C18 column (100x 2.1 mm, 1.7 µm) from Waters (Milford, MA, USA) and equipped with photodiode array detector (PDA). The gradient elution buffers were A (1% TFA in water) and B (1% TFA in acetonitrile). The gradient method was: 0-1 minutes, isocratic at 100% A; 1–10 minutes, gradient to 20% A; 10–11 minutes, gradient to 100% A; 11–14 minutes of stabilization at 95% A. The UV detector wavelength was set at 254 nm and the injection volume was 10 µL. Total run time was 14 minutes while the flow rate was set at 300 $\mu L \cdot min^{-1}$.
The mass spectrometry detection was carried out using a time-of-flight mass spectrometer (ESI-TOF) LCT Premier XE from Waters (Milford, MA, USA) with an electrospray ionization source, working in positive/V mode. The MS range acquired was between m/z 50–1.000. The capillary and cone voltages were set at 3.000 and 50 V, respectively. Desolvation gas temperature was 300 °C and source temperature was 120 °C. The desolvation gas flow was set at 600 $L \cdot h^{-1}$ and cone gas flow was set at 50 $L \cdot h^{-1}$. For quantification and data analysis, Masslynx v4.1 software was used (Waters, Milford, MA, USA). All the analytes were identified by mass spectrometry.

SEM and EDX. The morphology and composition of **1-FMN@AGM** samples before and after irradiation and their respective controls were examined using a field emission scanning electron microscope (FE-SEM) of Carl Zeiss MERLIN™ coupled to an Oxford Inca EDX system.

Inductively coupled plasma-mass spectrometry (ICP-MS). ICP-MS analysis for skin permeation experiments were carried out in He mode on a Thermo Fisher iCap-Q ICP-MS spectrometer equipped with a He gas kinetic energy discrimination (KED) collision/reaction cell. Calibration was done preparing solutions between 1 and 100 ppb of ^{195}Pt using the CMS-2 ICP-MS precious metal standard (10 ppm; Inorganic Ventures) using 3.6% v/v nitric acid (Optima grade, Fisher Scientific). ^{115}In (10 ppb) was used as internal standard, by adding 5 µl of the CGIN-1 ICP-MS standard (1000 ppm; Inorganic Ventures) to 500 ml of 3.6% v/v nitric acid (Optima grade, Fisher Scientific). Data processing was carried out using Qtegra™ software package (Thermo Fisher).
Agarose fractions were lyophilised, and then digested with 72% *v/v* nitric acid (1 mL; Optima grade, Fisher Scientific) on a Berghof Speedwave Xpert, Microwave Digestion System following the protocol:

Step	T (K)	P (bar)	Ramp (min)	Hold (min)	% Pot used
1	423	40	10	10	80
2	463	40	10	10	90
3	323	40	3	5	0

Samples were then diluted 20-fold using milliQ water to achieve a final concentration of 3.6% *v/v* nitric acid.

Cell culture. MCF-7 human breast adenocarcinoma cells were cultured as single monolayers at 37 °C in a humidified atmosphere containing 5% CO_2. For the task, we used high glucose Dulbecco's Modified Eagle Medium (DMEM) with sodium pyruvate and L-glutamine (Gibco; Reference: 41966029) supplemented with 10% foetal bovine serum (FBS) and 1% pencillin/streptopmycin. Cells were sub-cultured at regular intervals, and passages made by using 0.25% trypsin/EDTA when at 80–90% confluence.

Catalysis experiments. Unless otherwise specified, all catalytic reactions on **1-FMN@AGM** and their controls were carried out in air at 298 K using 10 mM Tris buffer (pH 7.6). Light irradiation experiments were performed employing an LED light source (λ_{max} = 460 nm, 6 mW·cm^{-2}). When GOX was included in the immobilized system, 1 M glucose was added to the photocatalytic reaction to trigger the oxygen depletion. After light irradiation, the beads were vacuum filtered and the supernatant was kept for further analysis. The filtered beads were incubated with 1 M NaCl in a ratio 1:10 (w:v) to desorb all the molecules ionically bound to the beads. Both reaction supernatants and NaCl elution samples were analysed by ^{1}H NMR and UPLC-MS to quantifying the amount of transformed **1** and the cisplatin produced. Integrations of the signals relative to the Pt-bound and free succinato ligand were used for monitoring the reaction progress via ^{1}H NMR. Cisplatin and **1** were identified and separated via UPLC-MS to quantify the Pt(IV)-to-Pt(II) conversion.

Single-particle fluorescence microscopy. 184 µL of 1:200 (w/v) suspension of **1-FMN@AGM** in 10 mM Tris-HCl buffer at pH 7.6 were placed into a well in an 8-well µslide. 36 µL of 0.1 mM NADH solution were added to trigger the reaction. The autofluorescence of NADH (λ_{ex}: 365 nm, λ_{em}: 402–448 nm) and **FMN** (λ_{ex}: 470 nm, λ_{em}: 500–557 nm) within each microbead was monitored every min for 1 h by using a Cell Axio Observer microscope with the Colibri LED illumination system incorporated. Images were then analyzed by using the software ImageJ.

MTT cell viability assay. MCF-7 cells were seeded in flat bottom 96-well plates (Corning) at densities of 5.000 cells per well, and left to adhere overnight. Then, they were treated with different concentrations of cisplatin or **1** (i.e. from 0.01 µM to 600 µM) for 48 h. Concentration

of the stock solutions used for the platinum complexes were determined by ICP-MS. We carried out cell viability experiments as duplicates of triplicates in independent experiments.
Alternatively, MCF-7 cells were seeded in 24 well plates (Corning) at densities of 30.000 cells per well, and left to adhere overnight. Next, they were treated for 48 h with: i) 5 or 10 µL aliquots of supernatant obtained by centrifuging light-irradiated (0 or 300 s) 50 µL Tris solutions containing 50 mg **1-FMN@AGM** or **1@AGM** (loading of **1** ≈ 3 µmol·g^{-1}, 0.15 µmol in total); or ii) lyophilized agarose deposited on Transwell® PET permeable supports (TC treated, diam. 6.5 mm, pore size 8.0 µm; Corning) containing the fraction of Pt released by **1-FMN@AGM** or **1@AGM** ointments and permeated through the STRAT-M membrane after light irradiation (0, 300 s). These experiments were carried out as duplicates or triplicates in independent experiments.
After the incubation period, the solutions of the Pt complexes were removed, and fresh media containing 0.5 mg/mL MTT (3-(4,5-dimethylthiazol-2-yl)-2,5-diphenyltetrazolium bromide) was added to each well (0.1 mL or 0.5 mL respectively for 96 and 24 well plates). The medium was removed again after 2 h, and the purple crystals formed were dissolved using DMSO. Finally, the absorbance of each well was measured at 550 nm (using 630 nm as reference) on a Tecan GENios Pro microplate reader, and plotted against an untreated control.

STRAT-M® membrane permeation experiments. 600 µL of hot liquid agarose (0.1% in TAE buffer) were deposited into each well of a 6-well transparent plate (Corning) and allowed to cool down and gel (Fig. S20a). On top of this agarose bed, we placed the STRAT-M® membrane (Merk, 25 mm) with the shiny side facing upward (Fig. S20b). Afterwards, 100 µL of Tris solution containing **1-FMN@AGM** and **1@AGM** were formulated with (1:1, v:w) polypropyleneglycol at 100 or 50%) to obtain a viscous solution that we spread on the STRAT-M® membrane (Fig. S20c). Next, wells were irradiated with blue light for 5 min with our custom-made LED light source (λ_{max} = 460 nm, 6 mW·cm^{-2}; Fig. S20d)[2] and the plate incubated in the dark overnight (18 h) to enable cisplatin diffusion through the synthetic membrane. Control samples were directly incubated in the dark without previous light irradiation. Afterwards, the STRAT-M® and the remaining **1-FMN@AGM** and **1-@AGM** suspensions were carefully removed to avoid contact with the agarose film at the bottom of the wells. These agarose portions collecting the permeated cisplatin were divided into two equal parts, lyophilized (Fig. S20e) and stored under refrigeration until use. We used one of the two halves for cell viability studies, while the other was digested with nitric acid in a microwave digestor (Berghof Speedwave Xpert) and used to determine the quantity of Pt that diffused through the membrane by Inductively Coupled Plasma Mass Spectrometry (ICP-MS) (Fig. S20f).

2. Supplementary figures and table

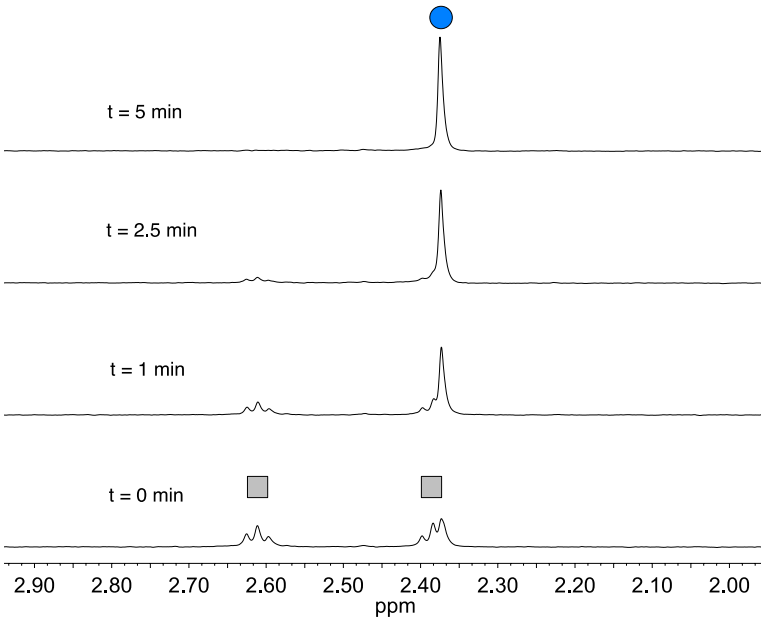

Fig. S1. Photocatalytic activation of **1**-**FMN**@**AGM** monitored by ^{1}H NMR. Spectra were collected in Tris/10% D_2O solution upon t = 0, 1, 2.5 and 5 min of 460-nm light irradiation (6 mW cm^{-2}), using the supernatant obtained after washing the beads with 1 M NaCl at each reaction time point. ^{1}H NMR signal labelling: **1**, ■ Pt–OCO**CH$_2$**CH$_2$CO$_2^-$, ■ Pt–OCOCH$_2$**CH$_2$**CO$_2^-$, ● free $^-$O$_2$C**CH$_2$CH$_2$**CO$_2^-$.

Table S1. Turnover Frequencies (TOFs, min^{-1}) for the photocatalytic activation of **1**-**FMN**@**AGM** with different catalyst loadings.‡

Irrad. time (min)	Offered FMN Load (μmol/g)	Loaded **1** (μmol/g)	Immobilized **1** (%)	Convers. to Cisplatin (%)	Converted **1** (μmol/g)	Experimental FMN Load (μmol/g)	TOF (min^{-1})
1	0.75	4.72	48.1±0.2	70.2±2.4	3.3±0.1	0.165	20.1±0.6
1	0.10	4.68	47.7±0.04	41.7±1.9	1.95±0.09	0.008	244±10

‡ 300 μL of **1**-**FMN**@**AGM** suspension with two different FMN loadings (1:10 with Tris buffer 10 mM pH 7.6) were placed into a filtration 96-well microplate and centrifuged at 3000 x g for 2 min in order to remove the buffer. The microplate was then irradiated with blue light for 1 min at 25 ºC. Afterwards, 300 μL of NaCl 1 M were added and incubated for 10 min. Finally, the microplate was centrifuged at 3000 x g for 2 min in order to collect the brine solution containing the released cisplatin and the unreacted **1**. UPLC-MS analysis was used to quantify the different components as previously described.

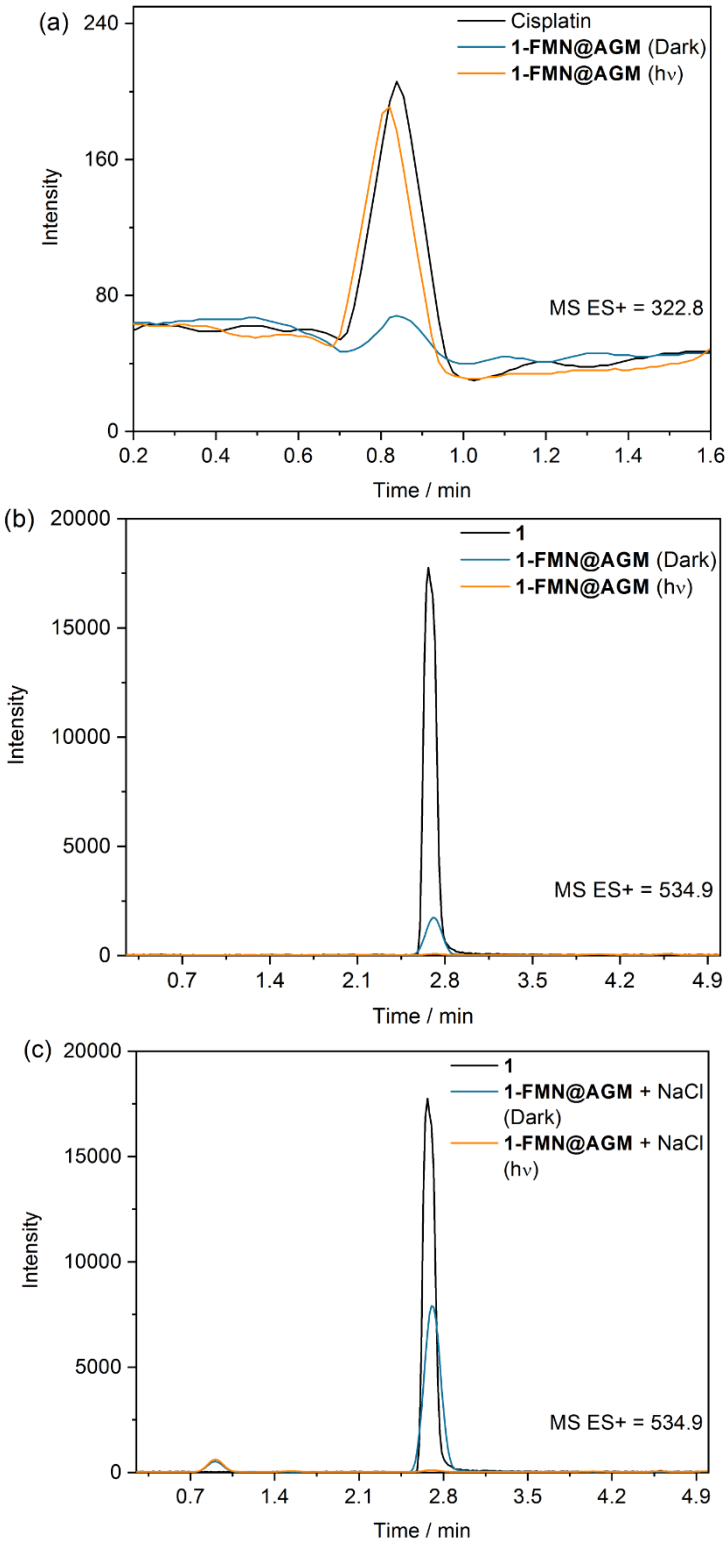

Fig. S2. UPLC-MS chromatograms of **1-FMN@AGM** in the dark and under light irradiation (10 min, 6 mW cm^{-2}). (a) Traces for cisplatin; (b) traces for **1**; (c) traces for **1** after washing with 1 M NaCl. Supernatant in the dark (dark cyan line); and supernatant after light irradiation (orange line). Standards for cisplatin and **1** (black lines) are added for comparison purposes. The chromatograms were exported to .csv file and plotted with the Origin software to obtain clearer and comparable graphs.

(a)

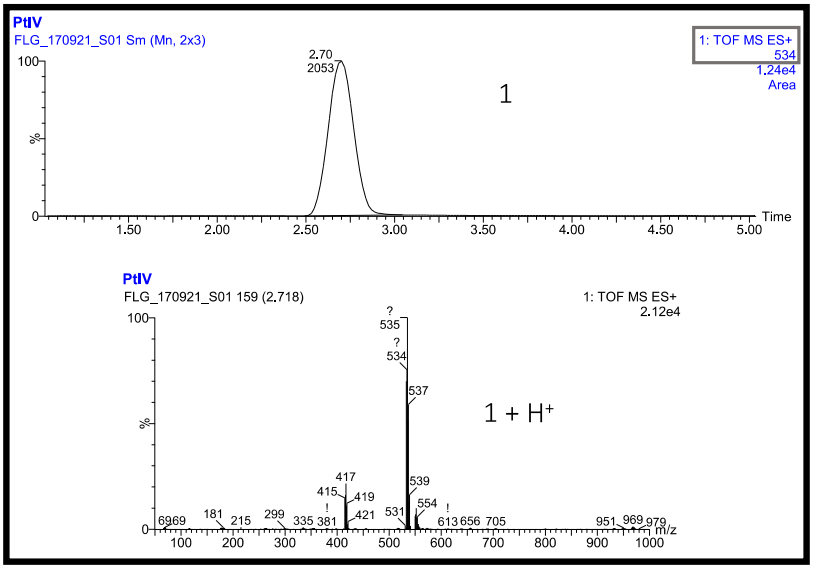
PtIV
FLG_170921_S01 Sm (Mn, 2x3)
1: TOF MS ES+
534
1.24e4
Area
2.70
2053
1
Time
PtIV
FLG_170921_S01 159 (2.718)
1: TOF MS ES+
2.12e4
1 + H+
m/z

(b)

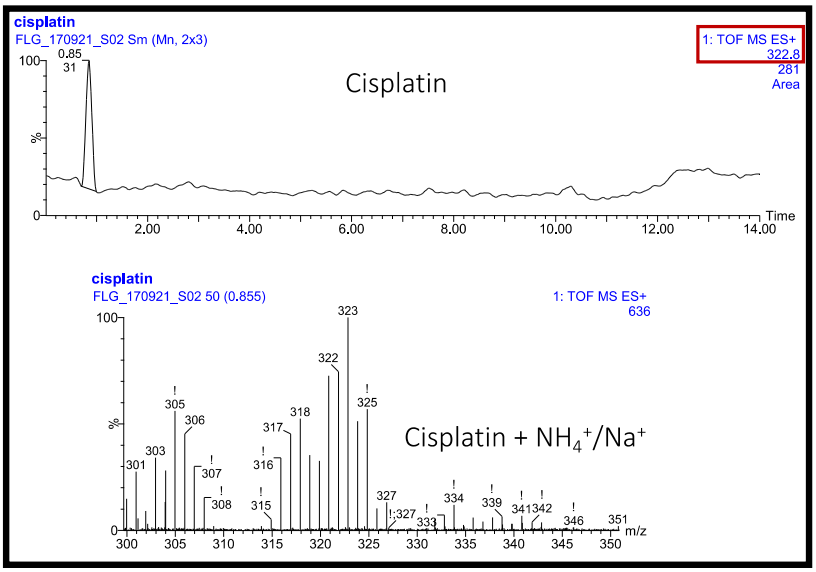
cisplatin
FLG_170921_S02 Sm (Mn, 2x3)
1: TOF MS ES+
322.8
281
Area
0.85
31
Cisplatin
Time
cisplatin
FLG_170921_S02 50 (0.855)
1: TOF MS ES+
636
Cisplatin + NH4+/Na+
m/z

(c)

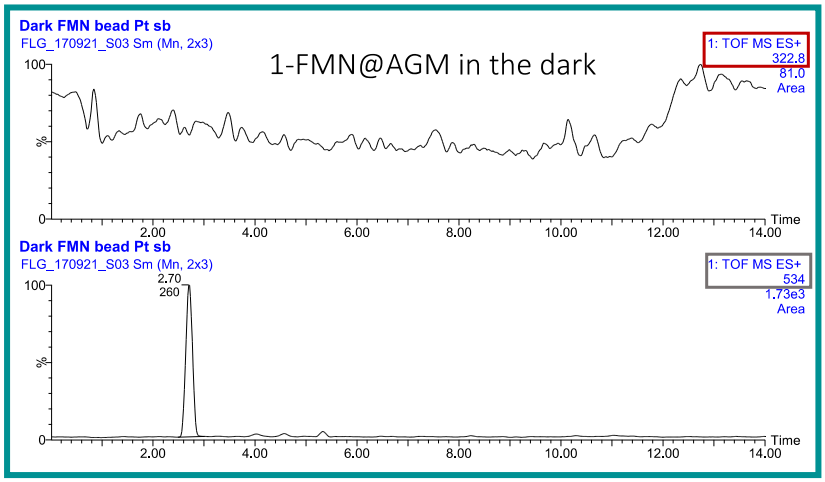
Dark FMN bead Pt sb
FLG_170921_S03 Sm (Mn, 2x3)
1-FMN@AGM in the dark
1: TOF MS ES+
322.8
81.0
Area
Time
Dark FMN bead Pt sb
FLG_170921_S03 Sm (Mn, 2x3)
1: TOF MS ES+
534
1.73e3
Area
2.70
260

(d)

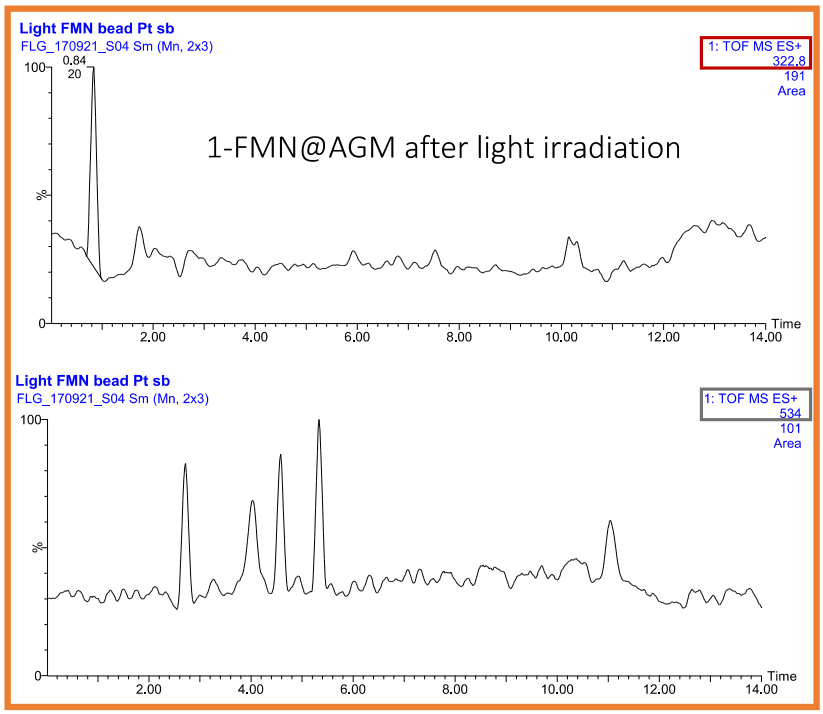
Light FMN bead Pt sb
FLG_170921_S04 Sm (Mn, 2x3)
1: TOF MS ES+
322.8
191
Area
0.84
20
1-FMN@AGM after light irradiation
Time
Light FMN bead Pt sb
FLG_170921_S04 Sm (Mn, 2x3)
1: TOF MS ES+
534
101
Area
Time

(e)

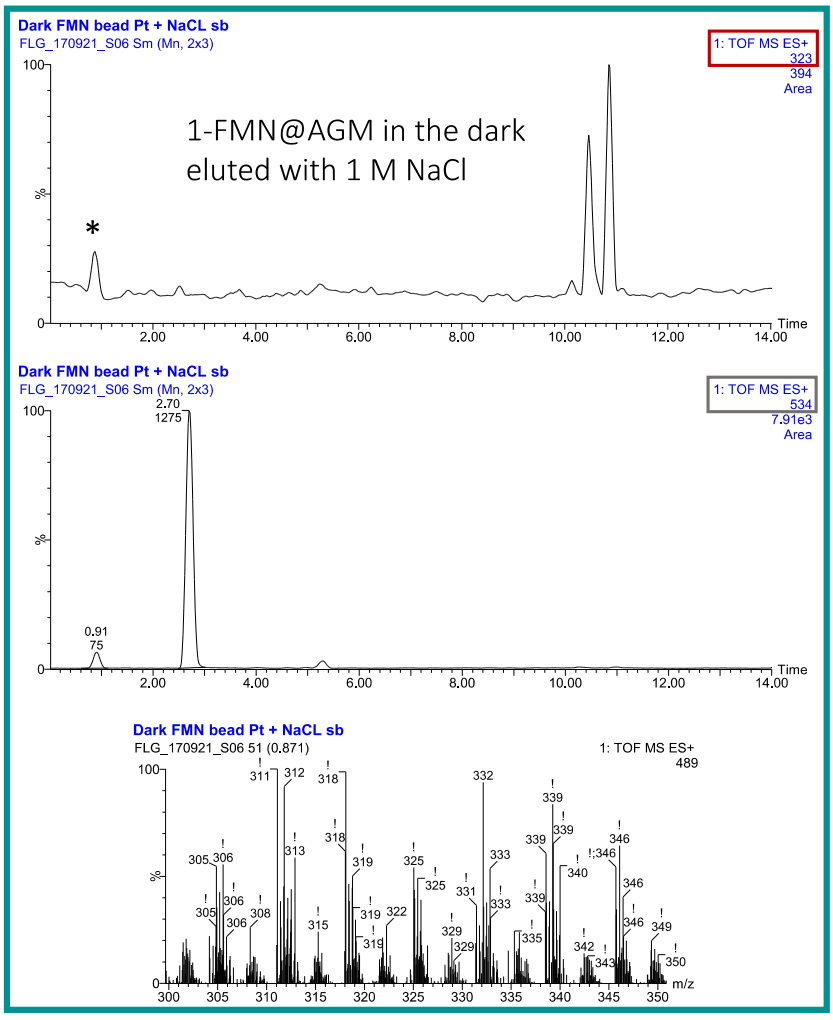
Dark FMN bead Pt + NaCL sb
FLG_170921_S06 Sm (Mn, 2x3)
1: TOF MS ES+
323
394
Area
1-FMN@AGM in the dark
eluted with 1 M NaCl
*
Time
Dark FMN bead Pt + NaCL sb
FLG_170921_S06 Sm (Mn, 2x3)
1: TOF MS ES+
534
7.91e3
Area
2.70
1275
0.91
75
Time
Dark FMN bead Pt + NaCL sb
FLG_170921_S06 51 (0.871)
1: TOF MS ES+
489
m/z

(f)

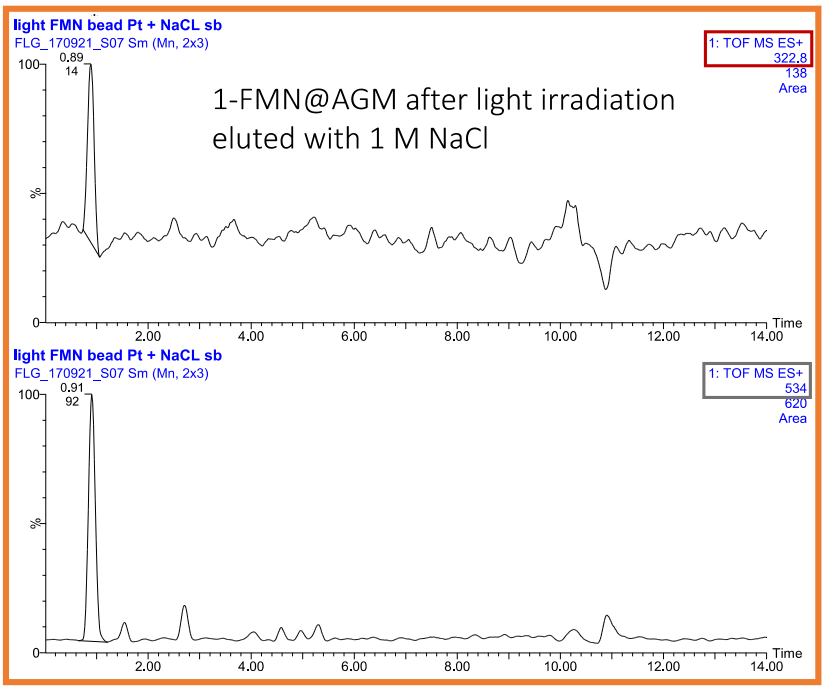

Fig. S3. Raw UPLC-MS chromatograms and MS spectra of: (a) Top trace: chromatogram of **1** (MS E+ 534.9). Bottom trace MS of peak at 2.7 min; (b) Top trace: chromatogram of cisplatin (MS E+ 322.8). Bottom trace MS of peak at 0.8 min; (c) **1-FMN@AGM** in the dark (top trace: chromatogram at MS E+ 322.8; bottom trace: chromatogram at MS E+ 534.9); (d) **1-FMN@AGM** after light irradiation (top trace: chromatogram at MS E+ 322.8; bottom trace: chromatogram at MS E+ 534.9); (e) **1-FMN@AGM** in the dark eluted with 1 M NaCl (top trace: chromatogram at MS E+ 322.8; middle trace: chromatogram at MS E+ 534.9; bottom trace: MS spectrum of an impurity at RT 0.85 min); (f) **1-FMN@AGM** after light irradiation and eluted with 1 M NaCl (top trace: chromatogram at MS E+ 322.8; bottom trace: chromatogram at MS E+ 534.9). *The impurity comes off the beads when they are incubated with NaCl.

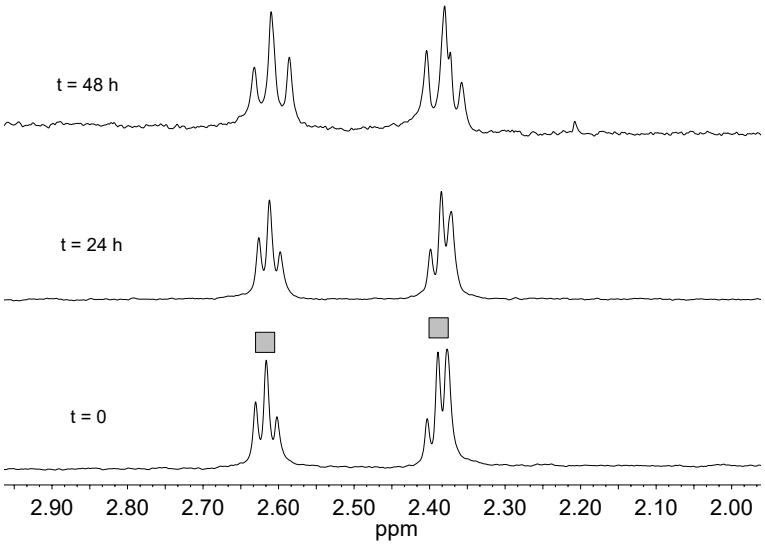

Fig. S4. Dark stability of **1** (1 mM) loaded into **AGM** monitored by ^{1}H NMR (Tris/10% D_2O pH 7.6). NMR spectra were measured after eluting the microbeads with 1M NaCl. ^{1}H NMR signal labelling: **1**, ■ Pt–OCO**CH$_2$**CH$_2$CO$_2^-$, ■ Pt–OCOCH$_2$**CH$_2$**CO$_2^-$.

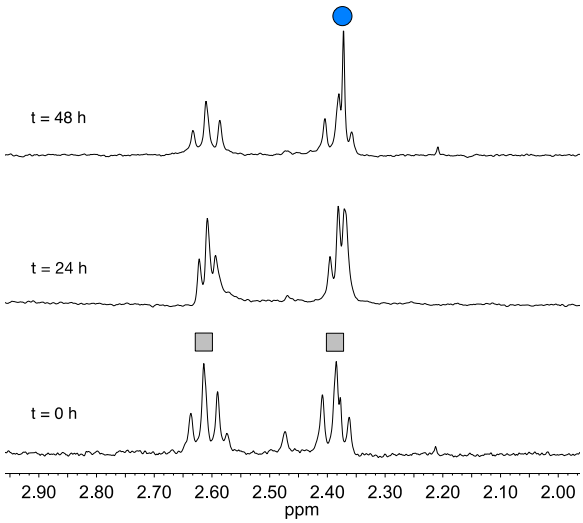

Fig. S5. Dark stability of **1** (1 mM) loaded into **AGM** in the presence of **FMN** (75 µM) and monitored by ^{1}H NMR (Tris/10% D_2O pH 7.6). NMR spectra were measured after inducing release of the microbeads content by NaCl (1 M). ^{1}H NMR signal labelling: **1**, ■ Pt–OCO**CH$_2$**CH$_2$CO$_2^-$, ■ Pt–OCOCH$_2$**CH$_2$**CO$_2^-$; ● free $^-$O$_2$C**CH$_2$CH$_2$**CO$_2^-$.

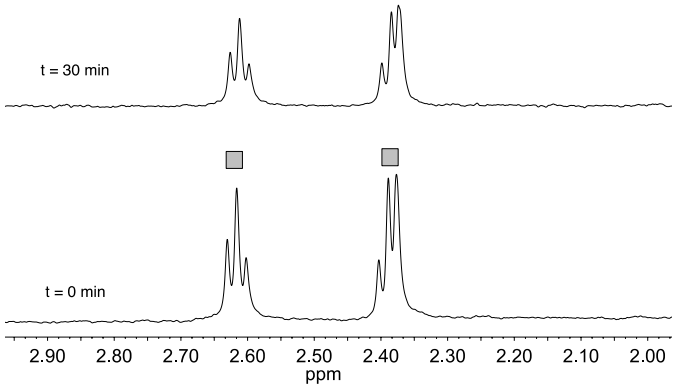

Fig. S6. Photostability of **1** (1 mM) loaded into **AGM** monitored by ^{1}H NMR (Tris/D_2O pH 7.6). NMR spectra were obtained upon t = 0 and 30 min of 460-nm light irradiation (6 mW cm^{-2}) and measured after inducing release of the microbeads load by NaCl (1 M). ^{1}H NMR signal labelling: **1**, ■ Pt–OCO**CH$_2$**$CH_2CO_2^-$, ■ Pt–OCOCH$_2$**CH$_2$**CO_2^-.

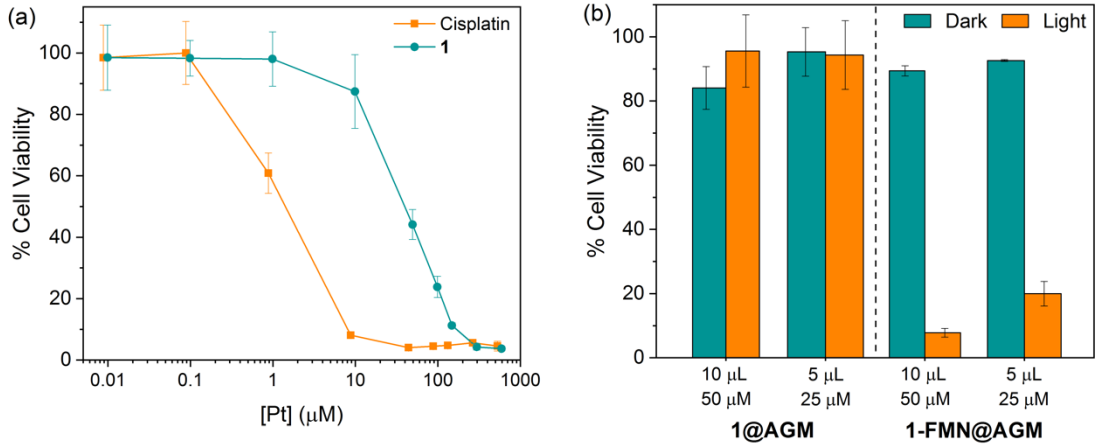

Fig. S7. (a) Cell viability of MCF-7 cells upon incubation with cisplatin and **1**. (b) Cell viability of MCF-7 cells following exposure to supernatant aliquots of **1@AGM** and **1-FMN@AGM** incubated in HEPES solutions in the dark and upon light irradiation (460 nm, 5 min). The X-axis reports the volume of supernatant added to 200 μL of cell culture medium and the corresponding estimated concentration of Pt species.

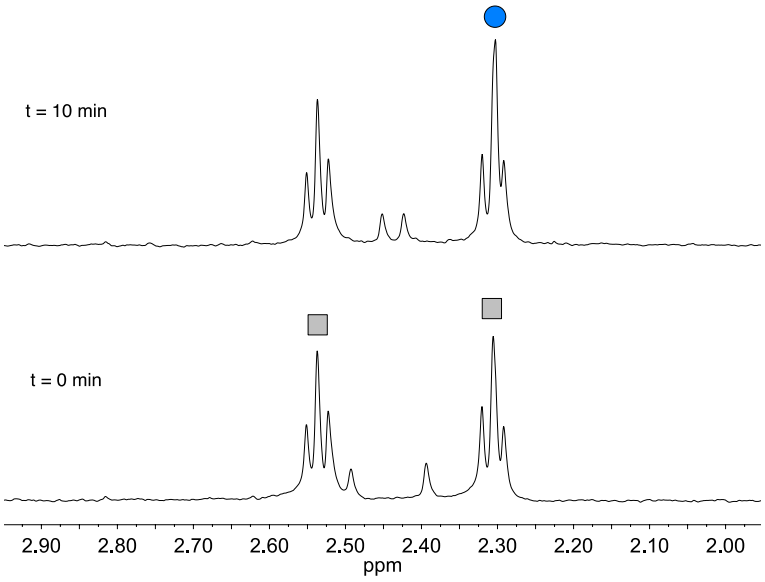

Fig. S8. Photostability of **1** in the presence of **FMN** monitored by ^{1}H NMR. Spectra were obtained for a Tris/D_2O solution of 1 mM **1** and 75 µM **FMN** upon t = 0 and 10 min of 460-nm light irradiation (6 mW cm^{-2}). ^{1}H NMR signal labelling: **1**, ■ Pt–OCO**CH_2**$CH_2CO_2^-$, ■ Pt–OCOCH_2**CH_2**CO_2^-, ● free ^-O_2C**CH_2CH_2**CO_2^-.

AGM – light irrad.

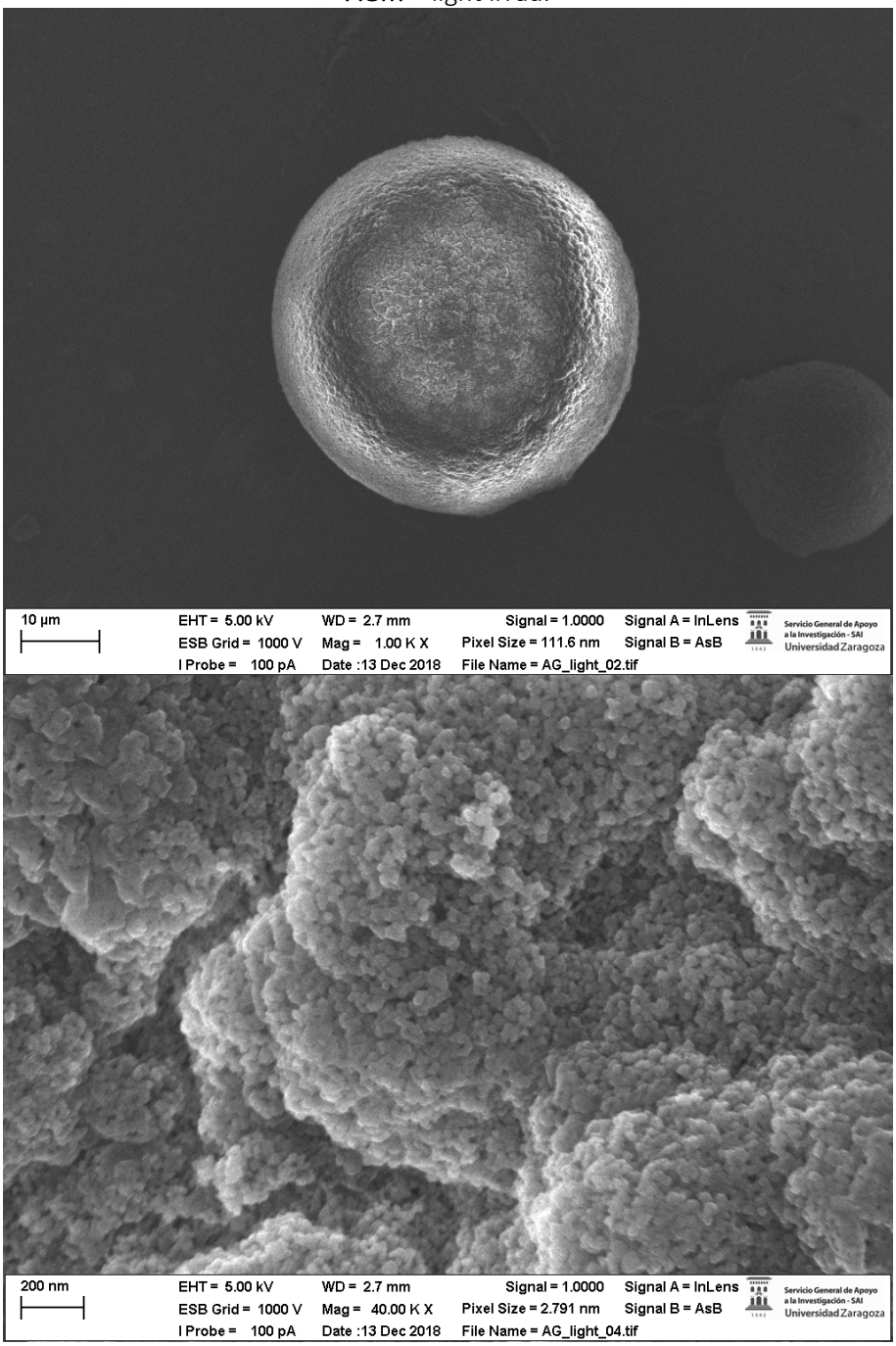

Fig. S9. Raw low (top) and high (bottom) magnification SEM micrographs of **AGM** under 460-nm light irradiation (6 mW cm^{-2}, 1 min).

1-FMN@AGM – dark

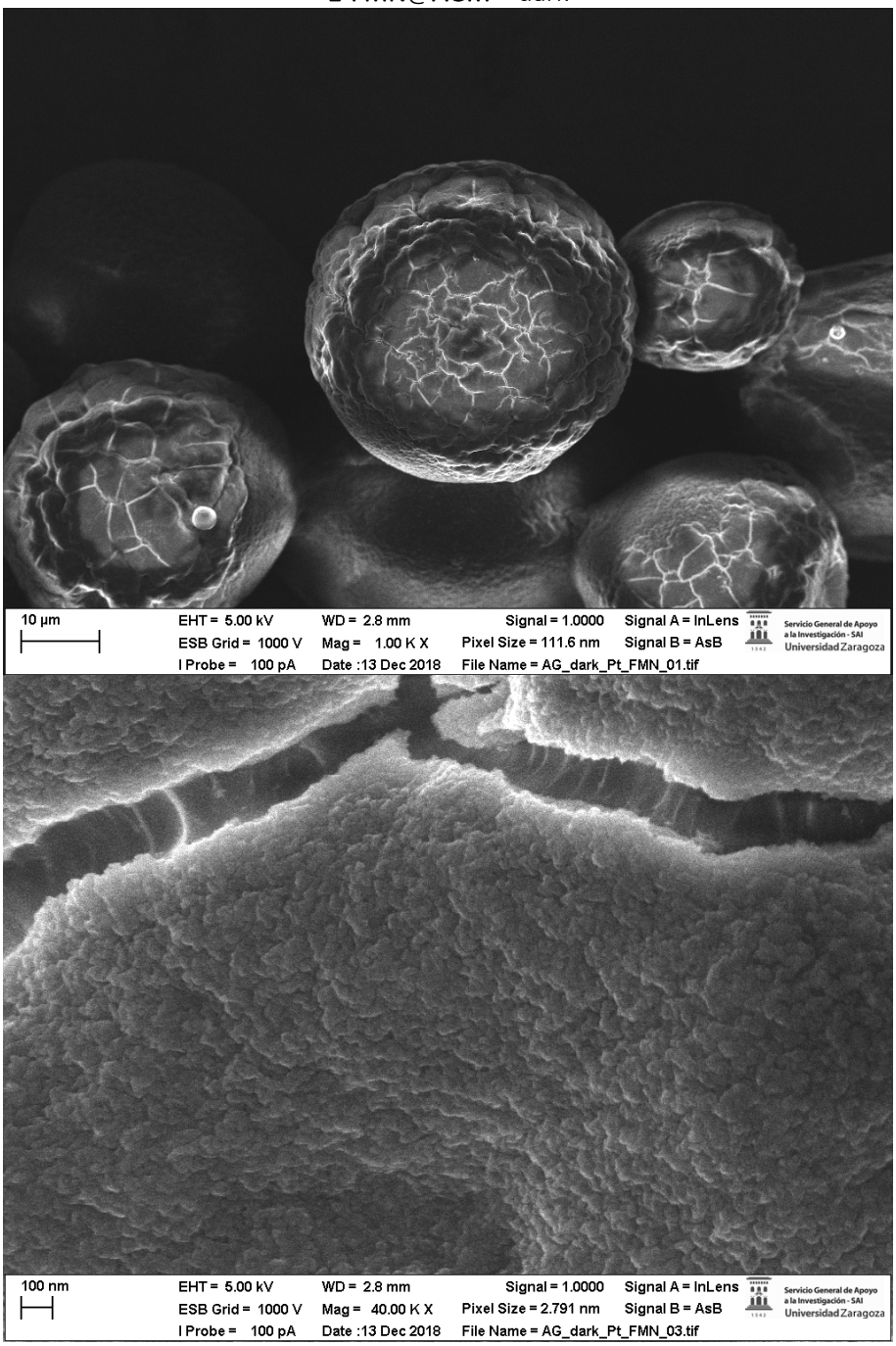

Fig. S10. Raw low (top) and high (bottom) magnification SEM micrographs of **1-FMN@AGM** in the dark.

1-FMN@AGM – light irrad.

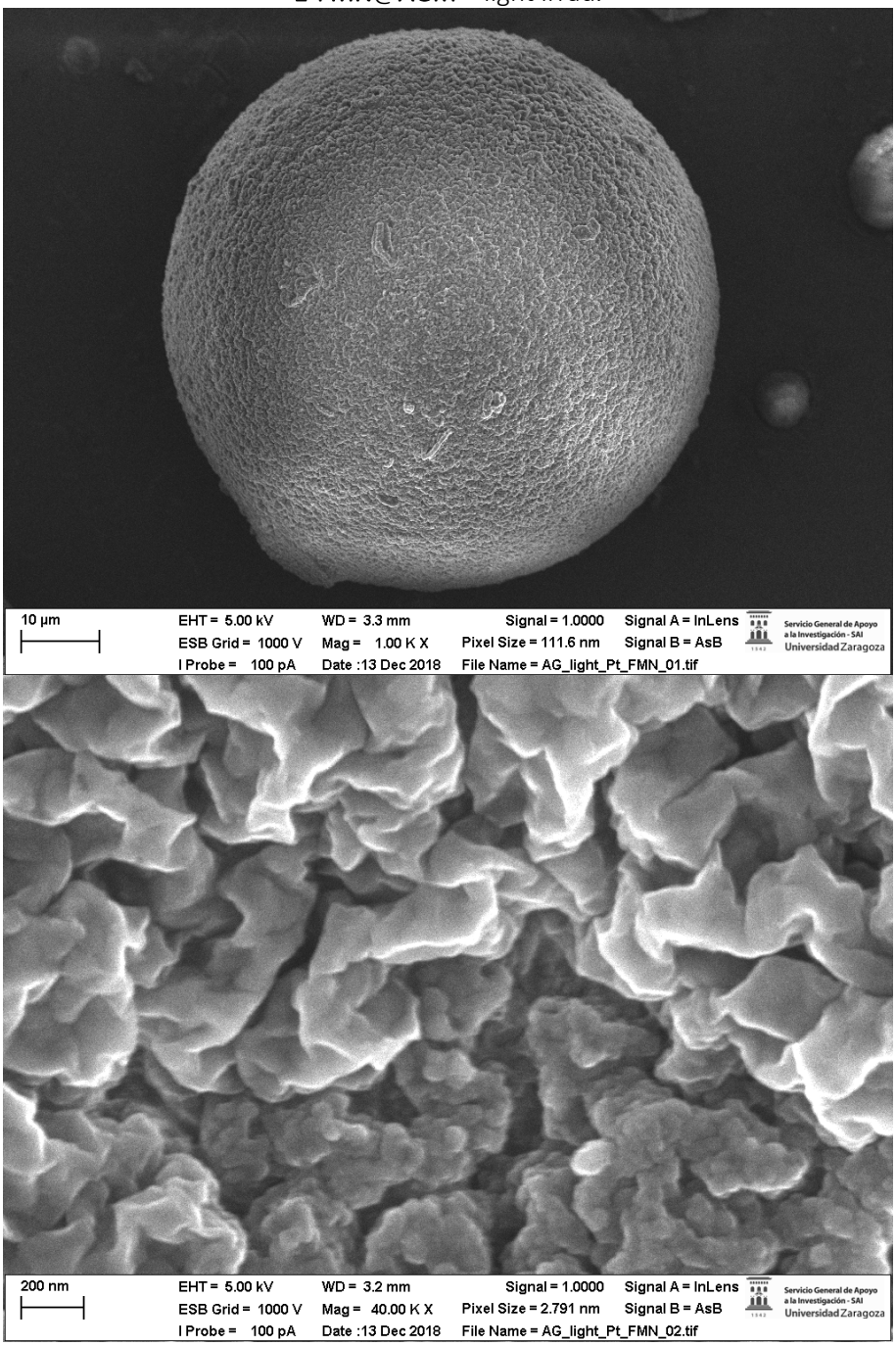

Fig. S11. Raw low (top) and high (bottom) magnification SEM micrographs of **1-FMN@AGM** under 460-nm light irradiation (6 mW cm^{-2}, 1 min).

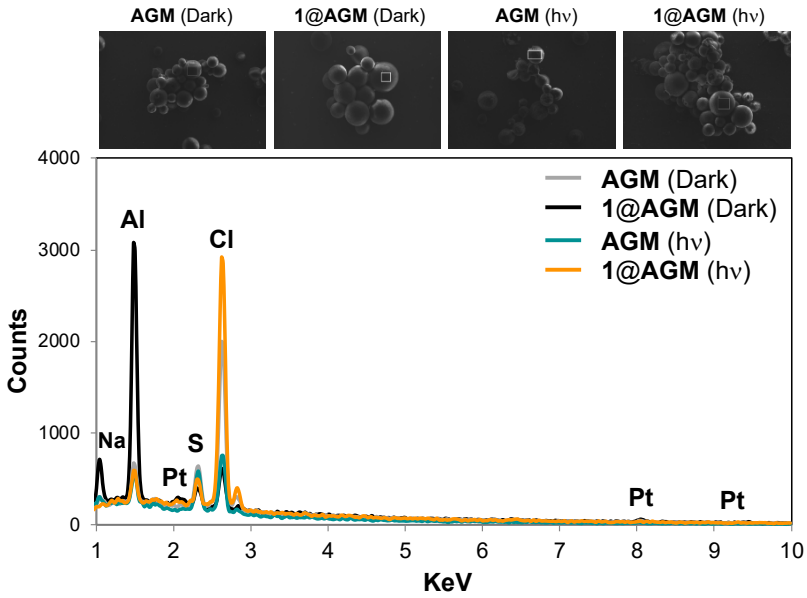

Fig. S12. EDX spectra **1@AGM** in the dark and (black line) upon light irradiation (orange line, 460 nm, 6 mW cm^{-2}, 1 min). The EDX spectrum of empty **AGM** was measured as control (dark: grey line; light-irradiated: dark cyan). EDX spectra ware collected from the sample region indicated by the squares in the lower magnification SEM micrographs.

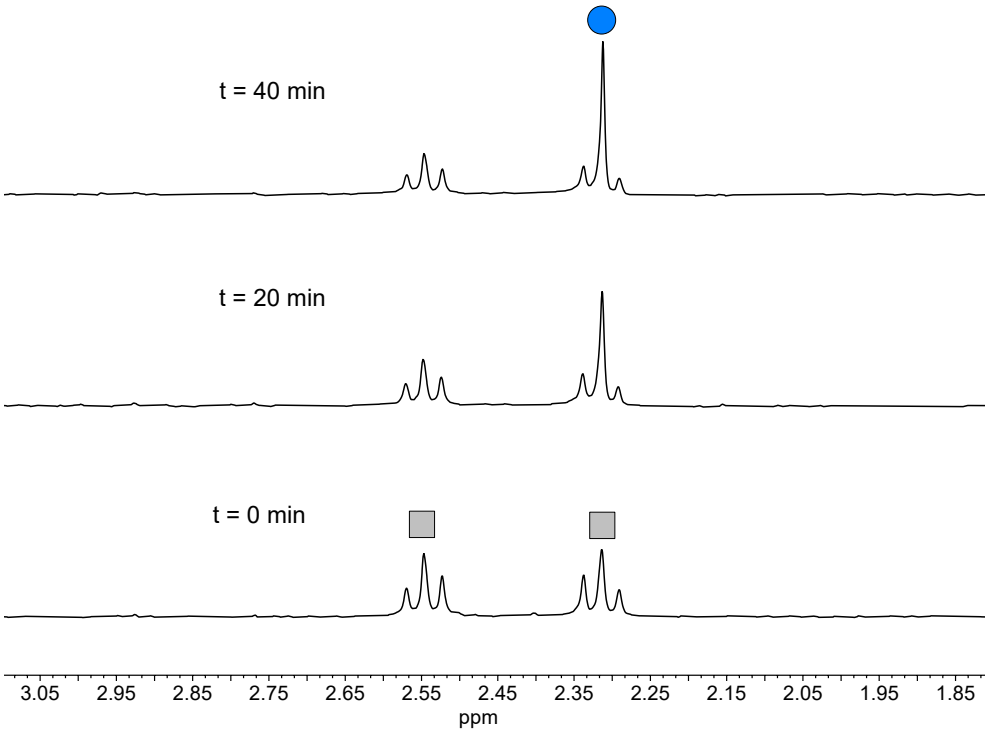

Fig. S13. Photocatalytic activation of **1** (0.5 mM) in the presence of **FMN** (25 μM) and diethylaminoethanol (2 mM) monitored by ^{1}H NMR. Spectra were collected in Tris/10% D_2O solution upon t = 0, 20 and 40 min of 460-nm light irradiation (6 mW cm^{-2}). ^{1}H NMR signal labelling: **1**, ■ Pt–OCO**CH_2**$CH_2CO_2^-$, ■ Pt–OCOCH_2**CH_2**CO_2^-, ● free ^-O_2C**CH_2CH_2**CO_2^-.

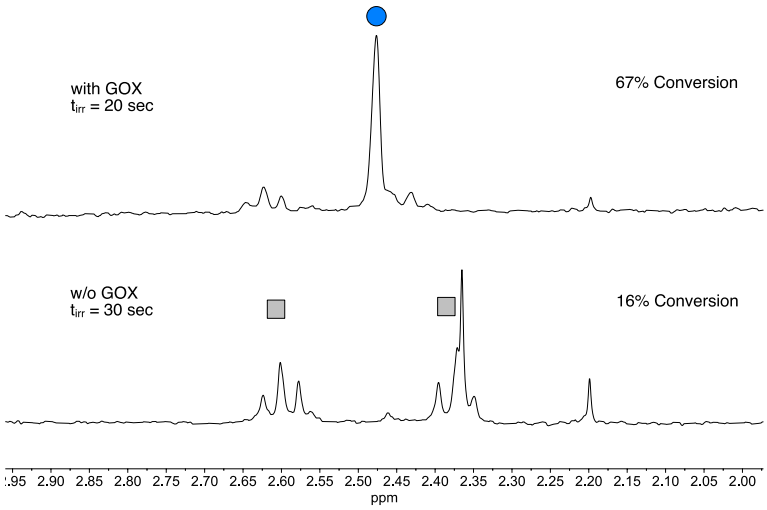

Fig. S14. Photocatalytic activation of **1-FMN-GOX@AGM** monitored by ^{1}H NMR. Spectra were collected in Tris/D_2O solution upon 20 s of 460-nm light irradiation (6 mW cm^{-2}), using the supernatant obtained after washing the beads with 1 M NaCl. ^{1}H NMR signal labelling: **1**, ■ Pt–OCO**CH$_2$**CH$_2$CO$_2^-$, ■ Pt–OCOCH$_2$**CH$_2$**CO$_2^-$, ● free $^-$O$_2$C**CH$_2$CH$_2$**CO$_2^-$.

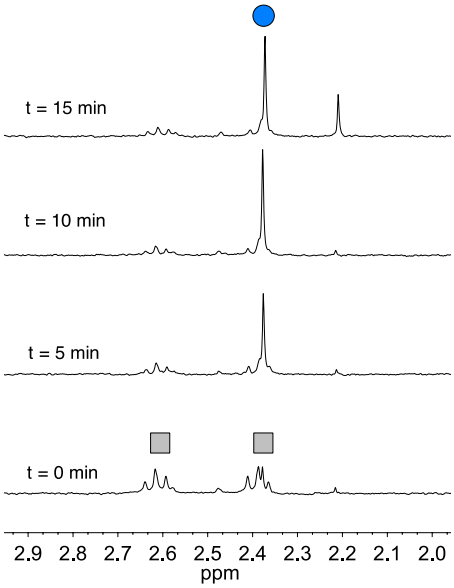

Fig. S15. NADH-triggered activation of **1-FMN@AGM** in the dark monitored by ^{1}H NMR. Spectra were collected in Tris/D_2O solution at t = 0, 5, 10 and 15 min of incubation with NADH (0.5 mM), using the supernatant obtained after washing the beads with 1 M NaCl at each reaction time. ^{1}H NMR signal labelling: **1**, ■ Pt–OCO**CH$_2$**CH$_2$CO$_2^-$, ■ Pt–OCOCH$_2$**CH$_2$**CO$_2^-$, ● free $^-$O$_2$C**CH$_2$CH$_2$**CO$_2^-$.

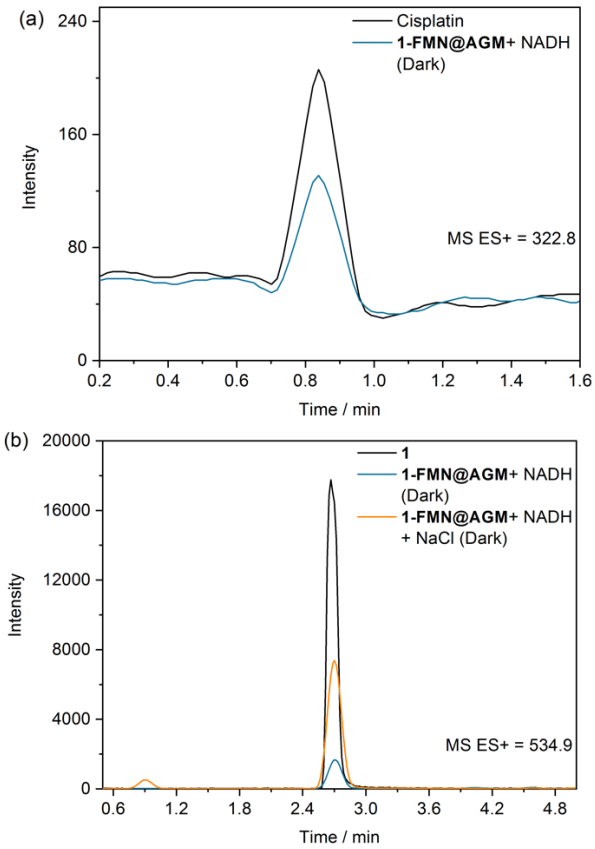

Fig. S16. UPLC-MS chromatograms of 1-FMN@AGM upon addition of NADH (0.5 mM) in the dark. (a) Traces for cisplatin; (b) traces for 1. Supernatant after addition of NADH, dark cyan line; and supernatant after addition of NADH and washing with 1 M NaCl, orange line. Standards for cisplatin and 1 (black lines) are added for comparison purposes. The chromatograms were exported to .csv file and plotted with Origin software to obtain clearer and comparable graphs.

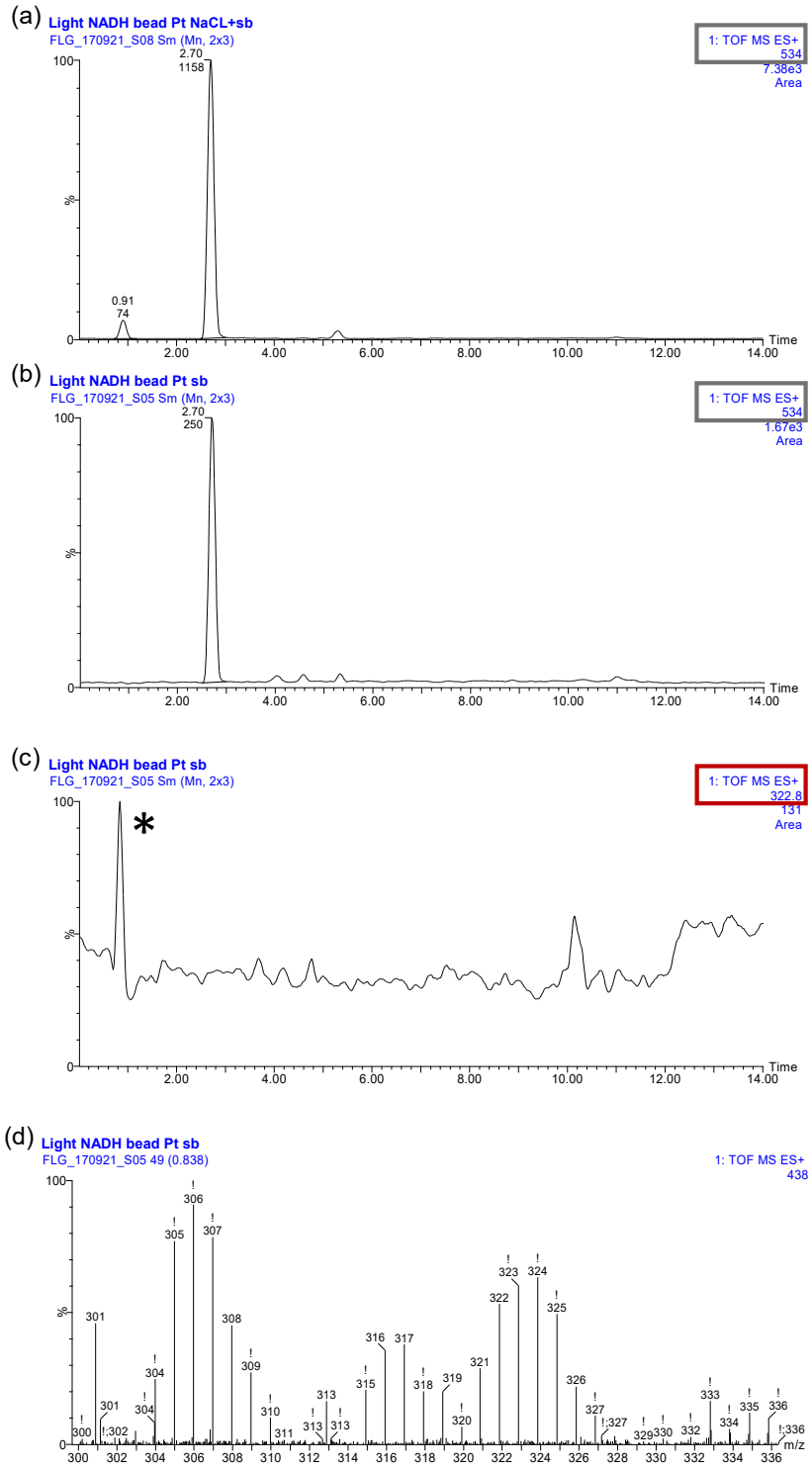

Fig. S17. Raw UPLC-MS chromatograms (a–c) and MS spectrum (d) of: (a) **1-FMN@AGM** + NADH in the dark (5-min incubation) and eluted with 1 M NaCl; (b) **1-FMN@AGM** + NADH in the dark (5-min incubation, chromatogram at MS E+ 534.9); (c) **1-FMN@AGM** + NADH in the dark (5-min incubation, chromatogram at MS E+ 322.8); (d) Mass spectrum of peak at RT 0.85 minutes (labelled as an asterisk)

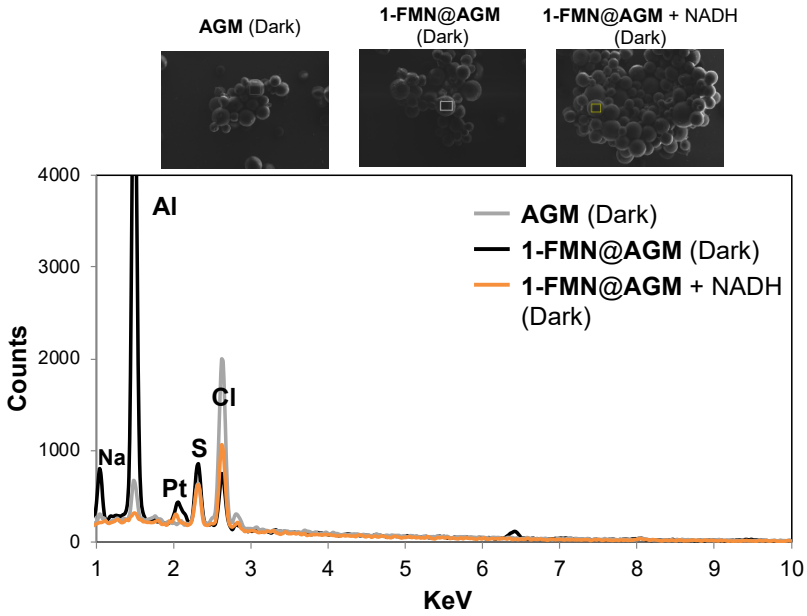

Fig. S18. EDX spectra **1-FMN@AGM** with (orange line) and without (black line) NADH incubation (10 min) in the dark. The EDX spectrum of empty **AGM** was measured as control (grey line). EDX spectra ware collected from the sample region indicated by the squares in the lower magnification SEM micrographs.

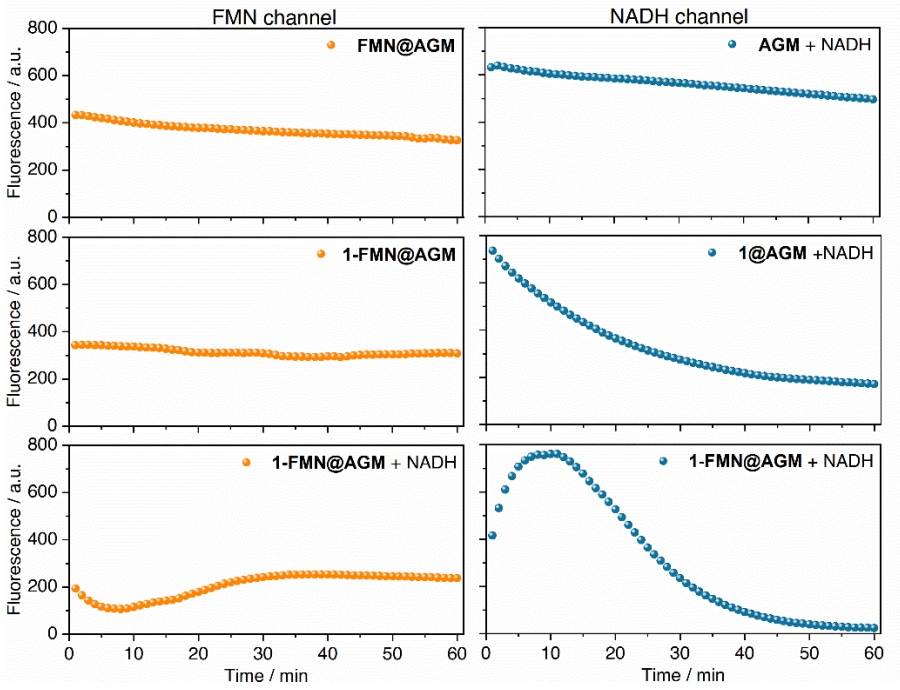

Fig. S19. Time-lapse fluorescence microcopy of **FMN** (orange dots: λ_{exc} = 470 nm, λ_{em} = 500–557 nm) and NADH (dark cyan dots: λ_{exc} = 365 nm, λ_{em} = 402–448 nm) immobilized on **AGM** with and without **1**. Time courses plots were created by analyzing and averaging the single-bead fluorescence intensity of at least 5 microbeads. Fluorescence values were obtained averaging 5 particles. ***Note***: in the NADH channel the fluorescence decay of the **1@AGM** + NADH sample indicates that some reactivity between **1** and NADH under UVA excitation (λ_{exc} = 365 nm) is occurring. This is not surprising since it was previously observed by Tanaka et al.[3] that NADH in the excited state undergoes photoinduced electron transfer to acceptors such as O_2. However, it is important to highlight that this species is not generated under blue light irradiation, hence in the catalysis conditions employed throughout this work.

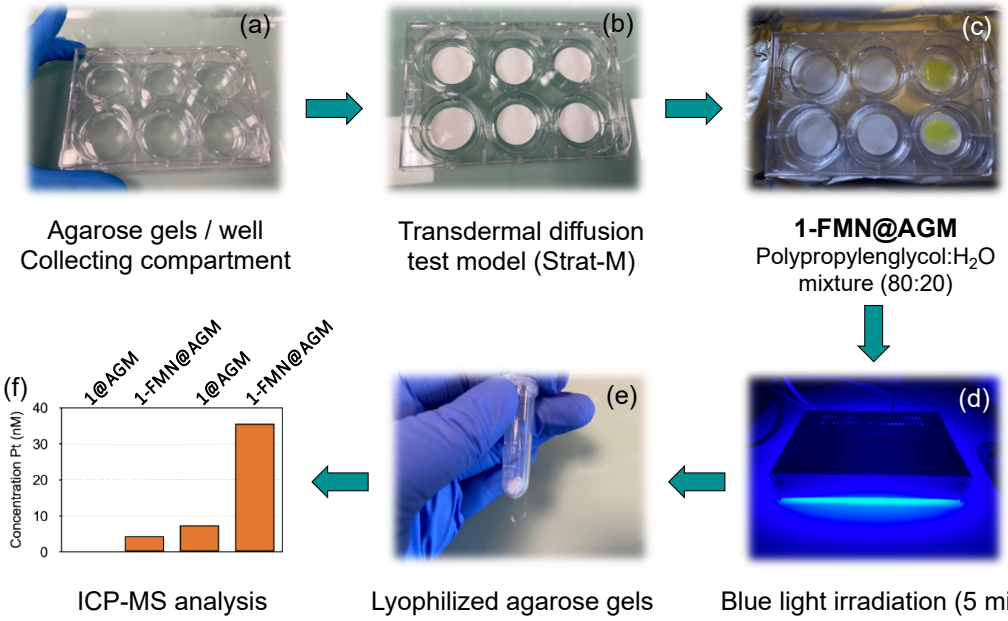

Fig. S20. Schematic representation of the experimental procedure adopted in the transdermal diffusion study of 1-FMN@AGM and controls using the STRAT-M synthetic membrane.

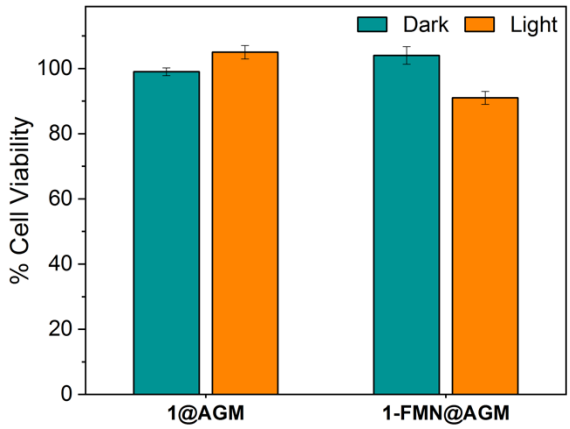

Fig. S21. Cell viability of MCF-7 cells treated with a portion of the lyophilized agarose containing the fraction of Pt released by 1-FMN@AGM or 1@AGM and permeated through the STRAT-M membrane after light irradiation (5 min) or incubation in the dark.

3. Supplementary references

1 P. Gramatica, E. Papa, M. Luini, E. Monti, M. B. Gariboldi, M. Ravera, E. Gabano, L. Gaviglio and D. Osella, *J. Biol. Inorg. Chem.*, 2010, **15**, 1157–1169.

2 S. Alonso-de Castro, E. Ruggiero, A. Ruiz-de-Angulo, E. Rezabal, J. C. Mareque-Rivas, X. Lopez, F. López-Gallego and L. Salassa, *Chem. Sci.*, 2017, **8**, 4619–4625.

3 M. Tanaka, K. Ohkubo and S. Fukuzumi, *J. Am. Chem. Soc.*, 2006, **128**, 12372–12373.